Cardiorespiratory Coupling Evaluation using Smart-Eyewear Technology: A Preliminary Study

Federica Mozzini[1], Sarah Solbiati[1], Sara Bernasconi[1], Alessandra Angelucci[1], Maria Antonella Lo Mauro[1], Andrea Aliverti[1], Diana Trojaniello[2], Enrico Gianluca Caiani[1,3]

[1] Politecnico di Milano, Electronics, Information and Bioengineering Dpt., Milan, Italy
[2] EssilorLuxottica, EssilorLuxottica Smart Eyewear Lab, Milan, Italy
[3] IRCCS Istituto Auxologico Italiano, Milan, Italy

Abstract

This study explores the feasibility of smart-eyewear (S-EW) technology to automatically extract cardiac and respiratory signals by head-ballistocardiography (H-BCG) and to assess cardiorespiratory coupling during a paced breathing protocol. In 7 healthy subjects, H-BCG was recorded using an inertial sensor integrated in the S-EW prototype. Simultaneously, ECG was acquired as a gold standard. After filtering, respiratory and cardiac components were derived to detect breathing cycles and heartbeats, enabling extraction of temporal and morphological parameters. A folded scattergram approach was applied to visualize changes in these parameters across the respiratory cycle, and differences between metrics were statistically evaluated. Respiratory cycle detection showed higher feasibility at respiratory rates of 6 and 8 seconds per respiratory cycle. Respiratory phase and rate dependences for both morphological and temporal H-BCG parameters were observed. These findings highlight the potential of S-EW technology for monitoring cardiorespiratory coupling in real-world scenarios, potentially including spontaneous breathing.

1. Introduction

Cardiorespiratory coupling (CRC) refers to the complex, linear and nonlinear dynamic interactions between the cardiovascular and respiratory systems, governed by multiple mechanisms, including respiratory sinus arrhythmia, cardio-ventilatory coupling, and respiratory stroke volume (SV) synchronization [1]. Understanding CRC is essential for assessing autonomic function and diagnosing cardiorespiratory disorders, as well as in the field of sports medicine to provide valuable insights into training effects, pre-competition stress, and physiological adaptations to various stimuli [2].

Research on CRC has explored different sensor placements for accurate monitoring. Chest-mounted inertial measurement units, including Micro-Electro-Mechanical Systems (MEMS), have been studied, with optimal results for both heart rate (HR) and breathing rate (BR) estimation when the sensor is positioned on the thorax around the mitral valve area, and for the dorsoventral direction [3]. The growing demand for wearable technologies for continuous health and fitness monitoring has driven interest in embedding MEMS in consumer wearables [4]. For MEMS positioned at the head level, the ability to detect from this head-ballistocardiographic (H-BCG) signal the respiratory-induced movements, as well as subtle micro-movements associated with cardiac activity, has been previously demonstrated by [5]. These micro-movements occur as each heartbeat propels approximately 12 grams of blood through the carotid arteries, generating cyclic head accelerations of about 10 mG (or 5 mm displacement) along the vertical axis [6].

In this context, smart eyewear (S-EW) technology is emerging as a promising tool for extracting physiological biomarkers such as HR and BR [7;8]. By embedding MEMS into the S-EW frame, it is potentially possible to continuously and unobtrusively monitor the H-BCG in real-world settings, thus resulting in a passive solution for long-term health tracking.

This preliminary study aims to evaluate the feasibility of assessing CRC by the H-BCG signal obtained by a S-EW during a controlled breathing protocol.

2. Materials and Methods

2.1. Study Population and Design

Seven healthy volunteers (2 women and 5 men; median (25th percentile; 75^{th} percentile) age: 25 (25;27) years; height 172 (164.5;179.5) cm; weight: 69 (63;78) kg) were recruited. The study protocol was approved by the Ethical Committee of Politecnico di Milano (n. 27/2023).

Tri-axial linear acceleration (A-P: antero-posterior, H-F: head-foot, R-L: right-left) and angular velocity (roll: around the A-P axis; pitch: around the R-L axis; yaw: around the H-F axis) were recorded using a MEMS (LSM6DSL module - ST Microelectronics, Montrouge, France) integrated into the left frame of a S-EW prototype (I-SEE, ©EssilorLuxottica,) at a sampling frequency of 100 Hz. Data from the S-EW were collected by Bluetooth using the Bluefruit Connect smartphone application (Adafruit Industries, New York, United States).

 ISSN: 2325-887X DOI: 10.22489/CinC.2025.303

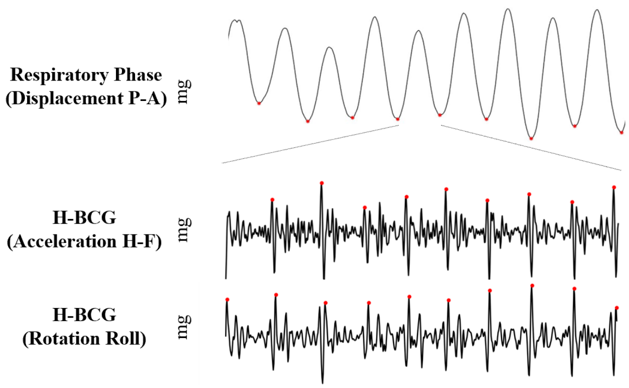

Figure 1: Top: respiratory signal obtained by the H-BCG during one phase of paced-breathing, where red dots indicate the start of each respiratory cycle. Bottom: corresponding cardiac activity signal obtained by the H-BCG (Acc. H-F and Roll), where red dots indicate the detected J peaks for each beat.

Simultaneously, a 1-lead ECG signal (sampling frequency 512 Hz) was recorded as a gold standard (Movesense Flash, Movesense Ltd., Vantaa, Finland), which also embeds a tri-axial MEMS (sampling frequency 208 Hz). The experimental protocol, with the subject in a seated position, included:

- 3 minutes free breathing ;
- paced breathing, guided by a recorded audio-guide [9], including 10 breaths at 4 seconds per respiratory cycle, 10 breaths at 6 sec, 10 breaths at 8 sec, and 10 breaths at 10 sec;
- four deep breaths followed by an apnoea at the end of inhalation (full lungs), and 3 minutes of recovery;
- four deep breaths followed by an apnoea at the end of exhalation (empty lungs).

At the beginning of the experiment, before sitting, participants were asked to perform a small jump to generate a motion artifact in the MEMS signals of both devices for synchronization purposes.

In this preliminary work, only signals acquired during the paced breathing phases will be utilized.

2.2. ECG and H-BCG Signal Processing

The ECG signal was pre-processed to remove noise and breathing-related motion artefacts using a 4th-order, zero-phase, band-pass Butterworth filter (0.5-30 Hz) [10]. Outliers were removed using the statistical method “grubs”, and the Pan-Tompkin algorithm was applied to extract the R peaks [11]. The RR intervals were computed as the time distances between consecutive R peaks.

The H-BCG signals were processed using two distinct methods to extract both cardiac and respiratory activity (Figure 1). For cardiac activity detection, signals of the H-F acceleration and roll rotations of the head were chosen [7], and band-pass filtered with 4th-order Butterworth (cut-off frequencies: 5 and 25 Hz [10]), to enhance intra-beat vibrations for subsequent beats identification. The J peak, corresponding to aortic valve opening, was detected beat-by-beat using an ECG-free algorithm [10] based on a template-matching technique [12].

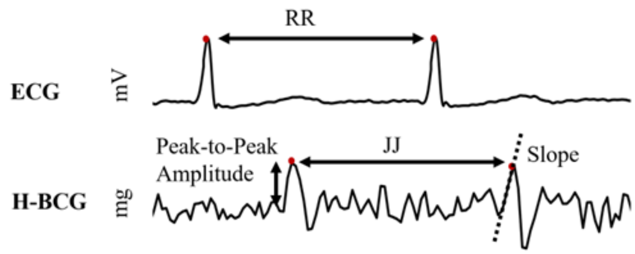

Figure 2. Morphological and temporal parameters computed on the ECG and H-BCG signals.

To minimize false positives, each J peak detection was compared with the previously identified R peaks, and considered valid if only one J peak occurred between consecutive R peaks. If >2 J peaks occurred between consecutive R peaks, the heartbeat was deemed invalid. In cases of two J peaks, the distance from each to its preceding R peak was compared to the median of all previous J-R intervals, retaining the J peak closest to the median and discarding the other one.

For respiratory activity, the displacement in the P-A direction of the H-BCG signal, computed through a double integration, was considered. Pre-processing included a 4th-order, high-pass Butterworth filter (0.1 Hz). The beginning and end of each paced-breathing phase in the protocol were identified by examining the derived respiratory signal. For each participant, each phase was qualitatively scored as excellent, good, or poor, depending on the ability to visualize the relevant 10 breathing cycles. Only respiratory phases classified as excellent were further analysed, by automatically detecting the beginning of each inspiration as the minimum of the respiratory signal. Then, based on the duration of each computed respiratory cycle, defined as the time difference between two minimum points, only breaths lasting within ±0.5 s of the expected imposed duration (4, 6, 8, or 10 s) were included in the analysis.

2.3. Computation of Temporal and Morphological Parameters

For each subject and phase, temporal and morphological parameters were calculated (Figure 2), including beat-to-beat duration from both the ECG (RR) and the H-BCG (JJ), the peak-to-peak amplitude difference between the J peak and the preceding minimum point and the corresponding slope (Slope). RR and JJ intervals were normalized for each subject and respiratory phase by their respective longest RR and JJ intervals. Similarly, morphological parameters, including peak-to-peak amplitude and slope, were normalized by the maximum amplitude or maximum slope, separately for each subject and respiratory phase.

	4 s/breath	6 s/breath	8 s/breath	10 s/breath
Respiratory cycles	2 [1;8]	6 [3;8]	6 [5;9]	4 [4;5]
Heartbeats -Acc. H-F	6 [3;24]	34 [17;43]	50 [42;64]	41 [31;49]
Heartbeats - Roll	10 [2;24]	31 [18;38]	40 [39;59]	37 [35;48]

Table 1: Feasibility analysis results for the four respiratory phases of the paced breathing protocol (median [25^{th}; 75^{th} percentile]). The first row reports the number of selected respiratory cycles for each respiratory phase. The second and third rows show the number of identified heartbeats per respiratory cycle in the acceleration H-F and roll axis, respectively.

2.4. Folded Scattergrams and Parameters

A folded scattergram (FS) is a graphical representation that visualizes changes in a parameter of interest, such as RR, according to the % of the respiratory cycle (0%: start of inspiration; 100%: end of expiration), as a cumulative representation over several breathing periods [13]. Each point on the FS corresponds to a specific value of the parameter of interest, with the y-coordinate representing the parameter's normalized value and the x-coordinate representing the timing of such event as % of the corresponding respiratory cycle [13]. For temporal parameters, such as RR and JJ intervals, the x-coordinate represents the midpoint between consecutive peaks.

Outliers were removed for each respiratory phase based on the median and the median absolute deviation (MAD) methods. The FS points were then fitted with sinusoidal harmonics in phase and quadrature, up to the third order, and the coefficients of the Fourier series were estimated by a least-squares algorithm [13]. The magnitude and phase of the first three harmonics were calculated.

To evaluate the representativeness of the sinusoidal fit to the points in the FS and the feasibility of evaluating the CRC, several figures of merit were computed: coefficient of determination (R^2) and its adjusted version (R^2 adj); from the Cosinor analysis [14], the acrophase (Φ), the ratio between the maximum amplitude (AO) and the midline of the oscillation (MESOR), along with the p-value of the Zero-Amplitude test; the median Euclidean distance and Nearest Neighbour distance.

2.5. Statistical Analysis

The effect of the imposed respiratory frequency phase was separately assessed on each computed temporal and morphological parameter using the Friedman test ($p<0.05$). If significant, post-hoc pairwise comparisons were applied to identify specific differences between phases (Wilcoxon Signed Rank test with Bonferroni Correction).

3. Results

3.1. Feasibility Analysis

Table 1 reports the number of respiratory cycles and heartbeats analysed for each protocol phase in both H-F acceleration and roll signals, highlighting a higher number of cycles when the duration was 6 or 8 seconds per breath (s/breath). Additionally, the number of identified heartbeats in the acc. H-F signal was consistently higher than in roll, reaching a 20% increase at 8 s/breath. As the number of analysable respiratory cycles in the 4-s/breath phase was very low, this phase was excluded from further analysis.

3.2. Folded Scattergram

Figure 3a shows the FS for temporal and morphological parameters obtained from one subject as an example. All parameters show a CRC, highlighting different behaviours and Φ in both temporal and morphological parameters.

3.3. Statistical Analysis

In RR and JJ intervals, as breath duration increased from shorter to longer, an increase in OA/MESOR and R^2, and a decrease in Nearest Neighbour Distance and p-value of the Zero-Amplitude test were noticed. Although this pattern is present overall, only OA/MESOR and R^2 exhibited significant differences between protocol phases, in RR and JJ intervals, respectively (Figure 3b).

The oscillation within the respiratory cycle of the morphological parameters was significantly more pronounced than that of the temporal parameters, as reflected in the higher OA/MESOR values. While a general pattern remains visible, fewer and non-significant differences were observed between the different protocol phases.

4. Discussion

We conducted a preliminary study to assess the feasibility of measuring CRC using cardiac and respiratory data acquired as H-BCG signal by S-EW technology. The results demonstrated the feasibility of the proposed approach during a paced breathing protocol with the subject in a seated position, highlighting that breath durations closer to physiological values (i.e., 6 and 8 s/breath) were more suitable for highlighting the phenomenon.

Changes in cardiac morphology and temporal parameters were visible at different % of the respiratory cycle and when measuring with S-EW. In particular, it

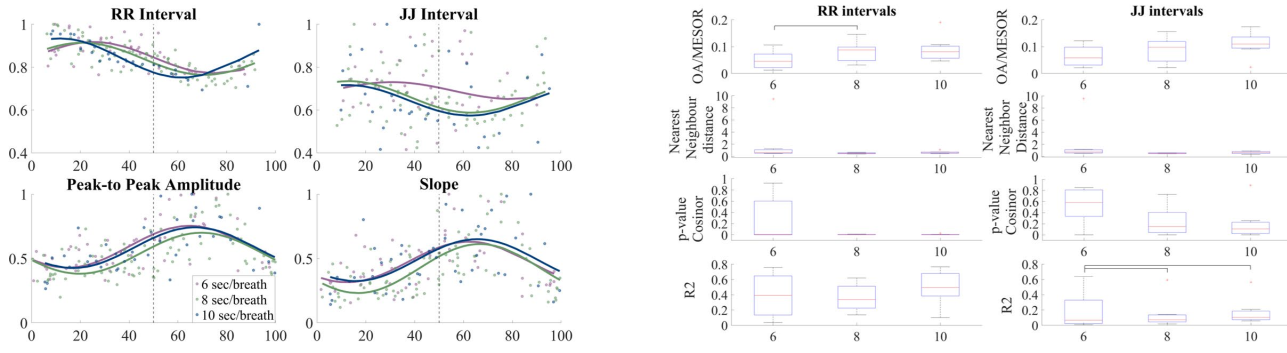

(a) (b)

Figure 3. (a) Folded scattergram of RR and JJ intervals, Peak-to-Peak amplitude, and Slope for a single subject on the acceleration H-F axis. The x-axis represents the percentage of the respiratory cycle [%], while the y-axis shows the normalized parameter values [0-1]. The vertical dotted line at 50% of the respiratory cycle represents the imposed end of exhalation-beginning of inhalation. Each coloured dot corresponds to a heartbeat within the respiratory cycle, and the coloured solid line represents the fitted function. Data is colour-coded: purple for 6 s/breath, green for 8 s/breath, and blue for 10 s/breath. (b) Boxplots of some of the parameters computed on the H-F axis on temporal parameters RR and JJ intervals. Horizontal lines indicate significant differences (p<0.05).

appears possible to visualize and quantify physiological Respiratory Sinus Arrhythmia from H-BCG using the JJ time series, in alignment with RR intervals, besides the noisier signal and a lower sampling frequency. Furthermore, the detected modulation in H-BCG Peak-to-Peak amplitude and Slope could be a potential correlate of respiratory-modulated preload and SV variations.

5. Conclusion

This work shows for the first time the feasibility of automatically measuring CRC when extracting cardiac and respiratory activity from MEMS embedded in S-EW technology, with the subject in a seated position during paced breathing, thus paving the way for future investigations during spontaneous breathing in real-life settings.

Acknowledgements

This work was carried out at the EssilorLuxottica Smart Eyewear Lab, a Joint Research Center between EssilorLuxottica and Politecnico di Milano.

References

[1] P. Balali et al., "Investigating cardiorespiratory interaction using ballistocardiography and seismocardiography—a narrative review," *Sensors*, vol. 22, no. 23, p. 9565, 2022.
[2] M. De Abreu et al., "On the significance of estimating cardiorespiratory coupling strength in sports medicine", *Frontiers in Network Physiology*, vol. *2*, 1114733, 2023
[3] C. Romano et al., "Investigation of Body Locations for Cardiac and Respiratory Monitoring With Skin-Interfaced Inertial Measurement Unit Sensors.", *IEEE Sensors Journal* 23, 7806-7815, 2023
[4] HS. Kang et al., "Wearing the future—wearables to empower users to take greater responsibility for their health and care: scoping review", *JMIR mHealth and uHealth*, vol. 10, no. 7, p. e35684, 2021
[5] C. Floris et al., "Feasibility of heart rate and respiratory rate estimation by inertial sensors embedded in a virtual reality headset", *Sensors*, *20*(24), 1–21, 2020
[6] G. Balakrishnan et al., "Detecting pulse from head motions in video", *Proceedings of the IEEE Conference on Computer Vision and Pattern Recognition*, pp. 3430-3437, 2013
[7] S. Solbiati et al., "Comparison of ECG-Free Algorithms for Heart Rate Computation From Head-BCG Signals Obtained With Smart Eyewear.", *MetroXRAINE*, pp. 213-218. IEEE, 2024
[8] J. Hernandez et al., "Cardiac and respiratory parameter estimation using head-mounted motion-sensitive sensors", *EAI Endorsed Trans. Pervasive Health Technol.*, vol. 1, no. 1, 2015
[9] A. Hossein et al., "Effects of acquisition device, sampling rate, and record length on kinocardiography during position-induced haemodynamic changes", *BioMedical Engineering OnLine*, vol. 20, pp. 1-18, 2021
[10] F. Landreani et al., "Assessment of ultra-short heart variability indices derived by smartphone accelerometers for stress detection", *Sensors*, vol. 19, no. 17, p. 3729, 2019
[11] J. Pan, W.J. Tompkins, "A real-time QRS detection algorithm", *IEEE Transactions on Biomedical Engineering*, vol. 3, pp. 230-236, 1985
[12] EG. Caiani et al. "Time-warping averaging for quantitative evaluation of changes in LV function," *Proceedings of the Joint 24th Annual Conference and Annual Fall Meeting of the Biomedical Engineering Society.*, vol. 1, IEEE, 2002.
[13] EG. Caiani et al., "Noninvasive quantification of respiratory modulation on left ventricular size and stroke volume." *Physiological measurement* 23.3: 567, 2002
[14] W. Nelson et al., "Methods for cosinor-rhythmometry", *Chronobiologia*, vol 6, pp: 305-23, 1979

Address for correspondence:
Prof. Enrico G. Caiani
Piazza Leonardo da Vinci, 32, Milan, 20133, Italy
enrico.caiani@polimi.it